

Uncertainty Propagation of Structural Computation for Fatigue Assessment

Ludovic Mell¹, Valentine Rey¹, Franck Schoefs¹ and Benjamin Rocher²

Received: 23 March 2022 / Accepted: 01 September 2022
© Harbin Engineering University and Springer-Verlag GmbH Germany, part of Springer Nature 2022

Abstract

Offshore wind substations are subjected to uncertain loads from waves, wind and currents. Sea states are composed of irregular waves which statistics are usually characterized. Irregular loads may induce fatigue failure of some structural components of the structures. By combining fatigue damage computed through numerical simulations for each sea state endured by the structure, it is possible to assess fatigue failure of the structure over the whole deployment duration. Yet, the influence of the discretization error on the fatigue damage is rarely addressed. It is possible to estimate the discretization error on the quantity of interest computed at the structural detail suspected to fail. However, the relation between this local quantity of interest and the fatigue damage is complex. In this paper, a method that allows propagating error bounds towards fatigue damage is proposed. While increasing computational burden, computing discretization error bounds is a useful output of finite element analysis. It can be utilized to either validate mesh choice or guide remeshing in case where potential error on the fatigue damage is too large. This method is applied to an offshore wind substation developed by Chantiers de l'Atlantique using two discretization error estimators in a single sea state.

Keywords Offshore wind turbines; Uncertainty propagation; Fatigue damage; Discretization error

1 Introduction

Deploying a structure at sea requires to ensure its structural safety. Waves, wind and current are uncertain phenomena that induce loads on the structure Veritas (2014). A few parameters, modelled as random variables, may describe these uncertain loads Bitner-Gregersen (2015). Loads resulting from each realization of these random variables may induce failure of the structure through different scenarios called limit states. Among these limit states, fatigue is a mechanical degradation that occurs when a structure endures a large number of local stress cycles that are below yielding but initiate micro-cracks in the component.

These cracks may propagate and induce failure of the structure. It usually arises at structural details concentrating stress such as weld toes. The initiation of crack is highly dependent on the microstructure of the material and the exact geometry of the structural detail.

To assess fatigue, a time series of the structural response (local stress) is usually computed for each sea state using discretized techniques such as the finite element method Veritas (1996). Then, rainflow counting is applied to the signal to isolate stress cycles Matsuishi & Endo (1968). S-N curves giving the number of cycles before failure from the stress amplitude allow to compute the fatigue damage, which is the inverse of the number of cycles before failure. Finally, the total damage is computed as the sum of individual damages for each stress cycle.

The number of cycles before failure is highly dependent on the microstructure of the material, the exact geometry of the structural detail and residual stresses from the welding process. It is therefore modeled as a random process. It is possible to include the geometry of the weld toe in the stochastic framework Pasqualini et al. (2013). Yet, this method is often too computationally expensive. Additionally, Paris law Paris (1961) allows assessing time dependent reliability of the propagation of cracks Soares & Garbatov (1996). For offshore structures, it is necessary to

Article Highlights

- A method is proposed for propagating error bounds towards fatigue damage and bounds on the probability of failure are derived.

✉ Valentine Rey
valentine.rey@univ-nantes.fr

¹ Nantes Université, École Centrale Nantes, CNRS, GeM, UMR 6183, F-44000 Nantes, France

² Chantiers de l'Atlantique, Avenue Bourdelle -CS90180, St-Nazaire CEDEX 44613, France

take into account the variety of stress cycles endured by the structure throughout its deployment. Therefore, the structural response has to be simulated for a lot of realizations of the sea states which may be computationally expensive. The use of a scatter diagram regrouping the probability of occurrence for ranges of the parameters describing the sea states allow to drastically reduce the number of simulations. Yet, it is sometimes insufficient in terms of computational cost reduction. Metamodeling the fatigue damage is a mean to reduce computational time (Casciati et al., 1992; Dong et al., 2018; Huchet et al., 2019). Then, the output of the fatigue analysis can be the probability that the cumulative damage exceeds a prescribed value.

A discretized technique such as the finite element method is widely used to solve the mechanical problem and obtain a time series of stress at the structural detail. Such technique introduces a discretization error. The coarser the mesh, the stiffer the structure and the smaller the probability of failure. Overestimating the structural capacity to endure loads may be dramatic. Furthermore, the mesh is generally chosen prior to fatigue analysis. Yet, it was proved in Ghavidel et al. (2018); Mell et al. (2020) that a small error on the local quantity of interest (i.e. local stress) can lead to a large error on the probability of failure. Therefore, the mesh has to be chosen in regards to the precision on the probability of failure. To this day, several techniques allowing to control the discretization error on the probability of failure exist. First, mesh convergence analysis can be performed on the probability of failure (Alvin, 2000; Demeyer et al., 2017; Ghavidel et al., 2020). However, it can lead to a huge computational cost as the probability of failure is computed for several meshes. Second, it is possible to use discretization error estimators that are available as a post-process of the finite element solution Zienkiewicz & Zhu (1987); Ainsworth & Oden (1997). Such techniques have been coupled with metamodeling techniques in Gallimard (2011); Mell et al. (2020). However, it was not applied to fatigue analysis. Indeed, the complex link between local stress and the fatigue damage does not allow to estimate directly the discretization error on the fatigue damage. In this paper, we propose a technique to propagate bounds computed on the local stress at the structural detail to the fatigue damage. It can be seen as a first step toward taking into account discretization error in the fatigue assessment of offshore structures using metamodeling techniques and standard recommendations from Veritas (1996).

First, the mechanical formulation and the computation of discretization error bounds on the local stress is introduced. Two estimators are used: one that is already available in some industrial codes but does not provide guaranteed error bounds and the other is more intrusive but provides guaranteed error bounds. Next, standard recommendations to compute the fatigue damage are presented. Then, methods to propagate discretization error bounds to-

ward the fatigue damage are proposed. Finally, the method is applied to the fatigue failure of a weld toe of an offshore wind substation. Moreover, inspection planning and digital twins of marine structures being highly based on fatigue computations, this method allows to quantify directly the uncertainty that can lead to bad decisions.



Figure 1 Offshore Gode Wind 3 electrical substation (©Chantiers de l'Atlantique)

2 Error bounds on the local stress of an offshore structure

2.1 Fatigue loads on an offshore wind substation

Wind is usually considered constant when modeling offshore wind substation environment. Therefore it does not induce fatigue in the structure. The surface of offshore wind substations exposed to wind is usually small. Also, currents are light at the deployment site. Therefore, the principal fatigue loads on these structures are mainly induced by waves. In order to assess fatigue failure of the structure, it is paramount to accurately describe the sea states composed of irregular waves. Significant wave height (H_s), peak period (T_p), main wave direction (θ_0), wave spreading function and wave spectrum model (usually chosen as one side Gamma model) are the principal parameters characterizing the sea states according to standards Veritas (2014). These parameters can be modelled as random variables. The statistics of the distribution of these random variables can be computed using *in situ* data (Bitner-Gregersen, 2015). Using a fully probabilistic approach to compute the fatigue damage of the structure is usually computationally expensive as the number of sea states to be simulated is excessively large. A scatter diagram giving the probability of occurrence for ranges of the triplet (H_s, T_p, θ_0) allows drastically reducing the number of sea states to be simulated compared to Monte-Carlo simulations. The statistics on fatigue loads are usually considered as converged when the sea state is approximately 3 h long. The fatigue damage for a full service of the offshore wind substation can be computed by extrapolating the damage in

each sea state using the estimated time that the structure will spend in each sea state according to the scatter diagram. Ideally, computational fluid dynamics should be used to compute wave induced loads on the structure. Because it is too computationally expensive, a 5th order Airy wave model used together with Morisson’s equations Sarpkaya (1986) are recommended practices Veritas (1996) to compute an analytical wave loads that may be integrated on the immersed structure as a boundary condition. It allows defining a mechanical problem that may be solved using a discretized technique such as the finite element method (FEM).

2.2 Mechanical formulation

In this subsection, we present the quasi-static mechanical problem. The finite element method allows solving a discretized version of the mechanical problem. We also present discretization error estimators that allow computing bounds on the local quantity of interest.

2.2.1 Continuous problem

Let \mathbb{R}^d represent the physical space and Ω the subspace of \mathbb{R}^d occupied by the structure (with d comprised between 1 and 3). This structure is subject to a body force \underline{f} on Ω , a traction force \underline{F} on its boundary $\partial_F \Omega$ and a displacement field \underline{u}_d on $\partial_u \Omega$. Let $\partial_u \Omega \cup \partial_F \Omega = \emptyset$ and $\partial_u \Omega \neq \emptyset$. The structure is assumed to undergo small perturbations and the unknown displacement field is denoted u . The symmetric part of its gradient is the deformation $\underline{\epsilon}(\underline{u})$. The material is considered to be linear elastic characterized by Hooke’s elasticity tensor \mathbb{H} . Let $\underline{\sigma}$ be the Cauchy stress tensor such that:

$$\underline{\sigma} = \mathbb{H} : \underline{\epsilon} \tag{1}$$

The mechanical problem may be written defining two affine subspaces, respectively kinematically and statically admissible:

$$KA = \left\{ \underline{u} \in (H^1(\Omega))^d, \underline{u} = \underline{u}_d \text{ on } \partial_u \Omega \right\} \tag{2}$$

and

$$SA = \left\{ \underline{\tau} \in (L^2(\Omega))_{\text{sym}}^{d \times d}; \forall \underline{v} \in KA^0, \int_{\Omega} \underline{\tau} : \underline{\epsilon}(\underline{v}) d\Omega = \int_{\Omega} \underline{f} \cdot \underline{v} d\Omega + \int_{\partial_F \Omega} \underline{F} \cdot \underline{v} dS \right\} \tag{3}$$

where KA^0 is defined with equation 2 for $\underline{u}_d = \underline{0}$. The error in constitutive relation is defined as a positive form:

$$e_{CR_n}(\underline{u}, \underline{\sigma}) = \left\| \underline{\sigma} - \mathbb{H} : \underline{\epsilon}(\underline{u}) \right\|_{\mathbb{H}^{-1}, \Omega} \tag{4}$$

where $\left\| \underline{x} \right\|_{\mathbb{H}^{-1}, \Omega} = \sqrt{\int_{\Omega} (\underline{x} : \mathbb{H}^{-1} : \underline{x}) d\Omega}$ Finally, the mechanical problem to solve reads:

Find a displacement field \underline{u}_{ex} and a stress field $\underline{\sigma}_{ex}$ such that:

$$\begin{aligned} & \text{On } \Omega, \begin{cases} \underline{\epsilon}(\underline{u}) = \frac{1}{2} (\underline{\text{grad}}(\underline{u}) + \underline{\text{grad}}(\underline{u})^T) \\ \text{div}(\underline{\sigma}) + \underline{f} = \underline{0} \\ \underline{\sigma} = \mathbb{H} : \underline{\epsilon}(\underline{u}) \end{cases} \\ & \text{On } \partial_u \Omega, \underline{u} = \underline{u}_d \\ & \text{On } \partial_F \Omega, \underline{\sigma} \cdot \underline{n} = \underline{F} \end{aligned} \tag{5}$$

An equivalent formulation of the mechanical problem may be written:

Find a couple $(\underline{u}_{ex}, \underline{\sigma}_{ex}) \in KA \times SA$, such that $e_{CR_n}(\underline{u}_{ex}, \underline{\sigma}_{ex}) = 0$

The solution to this problem $(\underline{u}_{ex}, \underline{\sigma}_{ex})$ exist and is unique. In most cases, this solution cannot be found analytically and the problem is usually discretized.

2.2.2 Discrete problem

Now let us discretize Ω into a tessellation Ω_h of triangles. The finite element method seeks a solution to the mechanical problem in a finite subspace $KA_h \subset KA$, where:

$$KA_h = \left\{ \underline{u} \in (H^1(\Omega))^d, \underline{u} = \underline{u}_d \text{ on } \partial_u \Omega_h \right\} \tag{6}$$

In practice, this subspace is generated by the *a priori* choice of a function basis of dimension m : $[\phi_i]_{i \in \llbracket 1, m \rrbracket}$

The discrete problem (also called forward problem) reads:

Find a couple $(\underline{u}_h, \underline{\sigma}_h)$ such that:

$$\begin{aligned} & \underline{u}_h \in KA_h \\ & \underline{\sigma}_h = \mathbb{H} : \underline{\epsilon}(\underline{u}_h) \\ & \forall \underline{v}_h \in KA_h^0, \\ & \int_{\Omega_h} \underline{\sigma}_h : \underline{\epsilon}(\underline{v}_h) d\Omega = \int_{\Omega_h} \underline{f} \cdot \underline{v}_h d\Omega + \int_{\partial_F \Omega_h} \underline{F} \cdot \underline{v}_h dS \end{aligned} \tag{7}$$

The solution of this discrete problem exists and is unique.

2.2.3 Computation of error bounds

Generalities The discrete solution \underline{u}_h usually does not coincide with the continuous exact solution \underline{u}_{ex} . We define the discretization error as $e_{discr} = \left\| \underline{u}_h - \underline{u}_{ex} \right\|_{\mathbb{H}, \Omega}$. An *a priori* estimate of this error may be computed when the conver-

gence rate of the FE problem is known. Some problem dependent constants that are not computable often make it impractical. *A posteriori* error estimators also exist. In that case, the finite element solution is post-processed to derive an estimation of the discretization error Ainsworth & Oden (1997). There are three families of *a posteriori* estimators of the discretization error. Some are based on stress smoothing techniques and provide an interval in which the exact solution should lie without guaranty Zienkiewicz & Zhu (1987). Some are based on residual and necessitate to compute problem dependent constants that are usually not computable. Assuming a value for these constants also make the error bounds not guaranteed. Finally, some techniques are based on the error in constitutive relation and provide guaranteed error bounds Ladevèze & Pelle (2005). In this paper, the stress smoothing technique is used for its cheapness, its easy implementation and its availability in some codes used in the industrial context (e. g. Abaqus). The estimator based on the error in constitutive relation is also used as it provides strict error bounds on the exact solution although being intrusive to the FEM code as the error estimator is not available in codes used in the industrial context.

Discretization error bounds based on a stress smoothing technique In this method, an admissible stress field is sought as an optimized stress field $\underline{\sigma}_{opt}$ by smoothing the finite element stress field $\underline{\sigma}_h$ (see Zienkiewicz & Zhu (1987)). To do so, the optimized stress field is decomposed in the same basis $[\phi_i]_{i \in [1, m]}$ as for the displacement \underline{u}_h . For each node j , the coefficients $[\sigma_{opt, i}^j]_{i \in [1, m]}$ are calculated by averaging the stress field on adjacent elements. An estimator of the discretization error is then obtained using:

$$e_{discr} = \left\| \underline{\sigma}_h - \underline{\sigma}_{ex} \right\|_{\mathbb{H}^{-1}, \Omega} \approx \left\| \underline{\sigma}_h - \underline{\sigma}_{opt} \right\|_{\mathbb{H}^{-1}, \Omega} \tag{8}$$

Discretization error bounds based on the error in constitutive relation Another technique provides strict upper bounds of e_{discr} (see Ladevèze & Pelle (2005)). Let us define the energy norm of the displacement $\|\cdot\|_{\Omega}$:

$$\|\underline{v}\|_{\Omega} = \left\| \underline{\varepsilon}(\underline{v}) \right\|_{\mathbb{H}, \Gamma} \tag{9}$$

The Prager-Syngé relation that is an adaptation of the fundamental Pythagore theorem for the norm $\|\cdot\|_{\Omega}$ reads:

$$\forall (\underline{\hat{u}}, \underline{\hat{\sigma}}) \in CA \times SA, \left\| \underline{\varepsilon}(\underline{u}_{ex}) - \underline{\varepsilon}(\underline{\hat{u}}) \right\|_{\mathbb{H}, \Gamma}^2 + \left\| \underline{\sigma}_{ex} - \underline{\hat{\sigma}} \right\|_{\mathbb{H}^{-1}, \Gamma}^2 = e_{CR_{\alpha}}^2(\underline{\hat{u}}, \underline{\hat{\sigma}}) \tag{10}$$

The displacement field $\underline{\hat{u}} = \underline{u}_h \in CA$ is kinematically ad-

missible. It can be used to obtain a bound on $e_{discr} = \underline{u}_{ex} - \underline{u}_h$:

$$e_{discr} = \|\underline{u}_{discr}\|_{\Gamma} \leq e_{CR_{\alpha}}(\underline{u}_h, \underline{\hat{\sigma}}) \tag{11}$$

The difficulty is to compute a statically admissible stress field $\underline{\hat{\sigma}} \in SA$. Several methods exist in that regard (see Ladeveze & Leguillon (1983), Parés et al. (2006), Pled et al. (2011) and Rey et al. (2014)).

Bounds on the quantity of interest The output of interest is rarely the displacement field \underline{u}_{ex} , but rather a quantity of interest $S(\underline{u}_{ex})$ that is local spatially. For offshore structures fatigue assessment, this quantity of interest is usually a stress component at a structural detail concentrating stress Veritas (2010). There are techniques to obtain bounds on the discretization error on the quantity of interest $S(\underline{u}_{ex}) - S(\underline{u}_h)$. When the quantity of interest is linear, it is possible to use extractors in the context of goal-oriented error estimation Becker & Rannacher (1996). For specific non linear quantities of interest, there are methods to calculate guaranteed bounds Strouboulis et al. (2000); Rüter & Stein (2006). If a specific method does not exist for a given non linear quantity of interest, it is possible to linearize it. Using extractors, we first need to define an adjoint problem:

$$\text{Find } \left(\underline{\tilde{u}}_{ex}, \underline{\tilde{\sigma}}_{ex} \right) \in CA^0(\Omega) \times \widetilde{SA}(\Omega) \text{ such that } e_{CR_{\alpha}}(\underline{\tilde{u}}_{ex}, \underline{\tilde{\sigma}}_{ex}) = 0 \tag{12}$$

where:

$$\widetilde{SA}(\Omega) = \left\{ \underline{\tau} \in (L^2(\Omega))_{sym}^{d \times d}; \forall \underline{v} \in CA^{00}(\Omega), \int_{\Omega} \underline{\tau} : \underline{\varepsilon}(\underline{v}) d\Omega = S(\underline{v}) \right\} \tag{13}$$

To solve the adjoint problem, it is possible to use the finite element method and obtain $\underline{\tilde{u}}_h$. Note that, the mesh does not need to be the same as for the reference problem. However, it would require an additional stiffness matrix factorization. The same mesh is used in this paper to save computational time as the resolution of the FE problem is simplified to a multiple (double) right-hand side linear system. Let us note $\underline{\hat{\sigma}}_h$ a statically admissible stress field built from $\underline{\tilde{u}}_h$ thanks to Ladeveze & Leguillon (1983), Parés et al. (2006), Pled et al. (2011) or Rey et al. (2014).

Exploiting the results from Ladevèze (2006, 2008), it is possible to derive an upper bound on the discretization error on the quantity of interest S . The linearity of S against the solution displacement field allows computing the discretization error on S as the product of the discretization error on the forward and adjoint problems. When using the

stress smoothing technique, it writes:

$$|S - S(\underline{u}_{ex})| < \left\| \underline{\underline{\sigma}}_h - \underline{\underline{\sigma}}_{opt} \right\|_{\mathbb{H}^{-1}, \Omega} \left\| \tilde{\underline{\underline{\sigma}}}_h - \tilde{\underline{\underline{\sigma}}}_{opt} \right\|_{\mathbb{H}^{-1}, \Omega} \quad (14)$$

It leads to the definition of an interval $[S^-, S^+]$ in which $S(\underline{u}_{ex})$ should lie:

$$\begin{aligned} S^+ &= S(\underline{u}_h) + \left\| \underline{\underline{\sigma}}_h - \underline{\underline{\sigma}}_{opt} \right\|_{\mathbb{H}^{-1}, \Omega} \left\| \tilde{\underline{\underline{\sigma}}}_h - \tilde{\underline{\underline{\sigma}}}_{opt} \right\|_{\mathbb{H}^{-1}, \Omega} \\ S^- &= S(\underline{u}_h) - \left\| \underline{\underline{\sigma}}_h - \underline{\underline{\sigma}}_{opt} \right\|_{\mathbb{H}^{-1}, \Omega} \left\| \tilde{\underline{\underline{\sigma}}}_h - \tilde{\underline{\underline{\sigma}}}_{opt} \right\|_{\mathbb{H}^{-1}, \Omega} \end{aligned} \quad (15)$$

For the error based on the error in constitutive relation, S^- and S^+ are found in a similar fashion as:

$$\begin{aligned} S^+ &= S(\underline{u}_h) - S_{hh} + \frac{1}{2} e_{CR_{\alpha}}(\underline{u}_h, \hat{\underline{\underline{\sigma}}}_h) e_{CR_{\alpha}}(\tilde{\underline{u}}_h, \hat{\underline{\underline{\sigma}}}_h) \\ S^- &= S(\underline{u}_h) - S_{hh} - \frac{1}{2} e_{CR_{\alpha}}(\underline{u}_h, \hat{\underline{\underline{\sigma}}}_h) e_{CR_{\alpha}}(\tilde{\underline{u}}_h, \hat{\underline{\underline{\sigma}}}_h) \end{aligned} \quad (16)$$

where $S_{hh} = \frac{1}{2} \int_{\Omega} (\hat{\underline{\underline{\sigma}}}_h + \mathbb{H} : \underline{\underline{\varepsilon}}(\tilde{\underline{u}}_h)) : \mathbb{H}^{-1} : (\hat{\underline{\underline{\sigma}}}_h - \mathbb{H} : \underline{\underline{\varepsilon}}(\underline{u}_h)) d\Omega$

Note that, in the case of the estimator based on the error in constitutive relation, $S(\underline{u}_h)$ is not guaranteed to lie in $[S^-, S^+]$.

2.2.4 Quantity of interest for offshore structures fatigue assessment

For the fatigue assessment of offshore structures, the quantity of interest is computed at a structural detail concentrating stress Veritas (2010). It is usually a weld toe between several structural components such as plates or tubulars (e.g. see Figure 2). Ideally, the whole weld toe should be inspected. It would require computing stress at every point on the weld toe which can be computationally intensive. To reduce computational burden, a few points are selected along the weld path and fatigue is assessed at each of them. Three recommended practices from Veritas (2010) allow calculating the local stress at the weld toe. The most accurate method would be to include the detail in the model. Such method is expensive computationally as it requires a fine mesh covering well the structural detail. The second method is based on the computation of the stress tensor at the point $N_{0.5}$, the point distant of $0.5 e$ from the weld toe, where e is the thickness of the plate that is welded. The stress tensor at the weld toe is then computed using a factor to account for local stress concentration. Finally, a linear extrapolation of the stress tensor from the points $N_{0.5}$ and $N_{1.5}$ to N_0 , is also possible. While any of the three methods presented here can be used, we will use a single point $N_{0.5}$ and a stress concentration factor for the ease of use of the technique.

In the basis $(\vec{e}_{\parallel}, \vec{e}_{\perp})$ represented in 2, the stress tensor

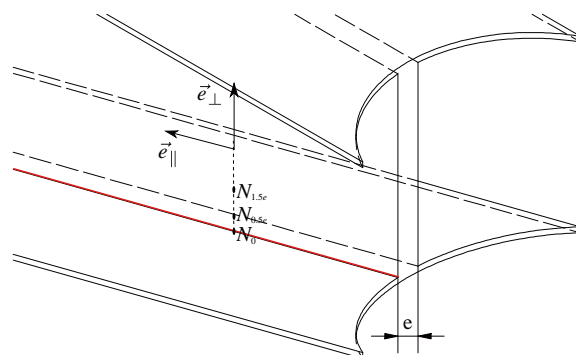


Figure 2 Zone of interest (weld toe in red) for the calculation of fatigue damage for a given structure

reads:

$$\underline{\underline{\sigma}}_{N_{0.5}} = \begin{pmatrix} \sigma_{\parallel} & \tau_{\parallel} \\ \tau_{\parallel} & \sigma_{\perp} \end{pmatrix} \quad (17)$$

The quantity of interest for further fatigue analysis is calculated as the maximal principal stress at % node $N_{0.5}$ with an extrapolation factor of 1.12 to account for the weld toe concentration:

$$\sigma_1 = 1.12 \max \begin{cases} a \left| \frac{\sigma_{\perp} + \sigma_{\parallel}}{2} + \frac{1}{2} \sqrt{(\sigma_{\perp} - \sigma_{\parallel})^2 + 4\tau_{\parallel}^2} \right| \\ a \left| \frac{\sigma_{\perp} + \sigma_{\parallel}}{2} - \frac{1}{2} \sqrt{(\sigma_{\perp} - \sigma_{\parallel})^2 + 4\tau_{\parallel}^2} \right| \end{cases} \quad (18)$$

where a is a constant depending on the quality of the welding process.

The quantity σ_1 is non linear against the differents stress components, obtaining error bound indicators is possible but more difficult. One can linearize this quantity of interest to compute error bounds, use quantity of interest dependent techniques or make an hypothesis on the direction of the maximal principal stress. In this paper a direction is assumed for the maximal principal as providing a σ_1 specific technique is out of the scope of this paper. This direction is assumed by expert knowledge given the geometry and the loads on the structure.

3 Computing fatigue damage from the time-series of stress

Before defining a new strategy to propagate bounds obtained on the quantity of interest toward the fatigue damage, it is necessary to elaborate on the method to compute the fatigue damage. The method that is used in this paper follows recommended practices from Veritas (2010). Giv-

en a time series of stress obtained with the finite element method, the rainflow counting algorithm proposed in Matsuishi & Endo (1968) is used to identify stress cycles $\Delta\sigma$ within the signal. Interested readers may refer to Veritas (2010) for an in depth explanation of rainflow counting.

A number of cycles before failure can be assigned to each $\Delta\sigma$ using an SN curve given by standards Veritas (2010). As shown in Figure 3, the SN curve is probabilistic as the weld toe properties have intrinsic variability.

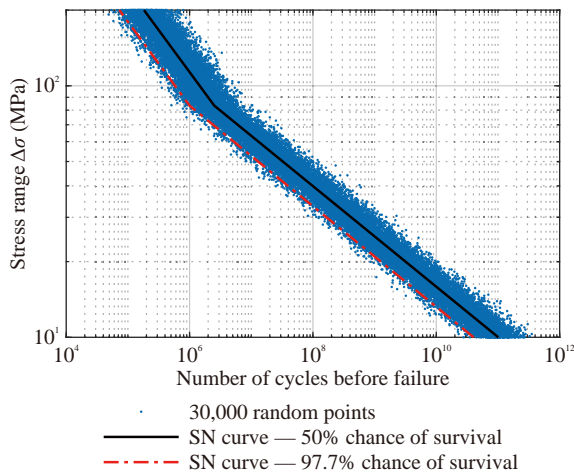


Figure 3 Stress to Number of cycles curves (SN-curves) - Parameters from the D-curve for a detail in seawater with cathodic protection in Veritas (2010)

4 Propagating bounds on stress toward fatigue damage

Using discretization error estimators through (15) or (16), a FEM solution $S(\underline{u}_h)$ and an interval $[S^-, S^+]$ may be obtained at each timestamp t_k ($k \in \llbracket 1, n_{ts} \rrbracket$) of the time series. It is significantly different from state of the art fatigue analysis for which a single value of stress is known. Propagating bounds on stress to the damage is not a trivial task. Taking into account rainflow counting and SN-curves, damage is sensitive to the range of fluctuation and the mean stress. We focus here on the range of fluctuation. Our main concern is the range of fluctuation considering that the more (respectively the less) a signal oscillates, the larger (respectively the smaller) the total damage. The more the mean value of the stress the more the total damage. We do not consider this issue that is easier to solve: we can compute the damage with the highest value of the mean value for the stress computation without bounds and for the two signals presented in the following. Based on this hypothesis, we propose to build two signals passing within each interval delimited by bounds:

- one maximizing damage and thus presenting maximum oscillation

- one minimizing damage and thus presenting minimal oscillations.

Signal minimizing damage Let the signal minimizing damage be the one passing for each time stamps t_k at the point within $[S^-(t_k), S^+(t_k)]$ which is the closest to the one selected for t_{k-1} . For t_0 , we select this point as the boundary $S^-(t_0)$ or (S^+t_0) closest to the first interval $[S^-(t > t_0), S^+(t > t_0)]$ guaranteed to be above or below the interval $[S^-(t_0), S^+(t_0)]$. An algorithm that allows building such signal is given in Algorithm 1.

An example of such signal is shown in Figure 4(b). The signal remains constant if the value selected at t_{k-1} lies in $[S^-(t_k), S^+(t_k)]$ which is necessary to minimise damage. Otherwise, it will pass by either $S^-(t_k)$ or $S^+(t_k)$. Note that it is not formally proved that this signal minimizes oscillation, yet it seems to be validated by observation.

Signal maximizing damage Two signals are proposed to build the signal maximizing damage. First, we propose to use the signal successively oscillating between S^- and S^+ during the time series. An algorithm that allows building such signal is given in Algorithm 2. Such signal is plotted in Figure 4(a). Note that this signal is rather unrealistic as the position of the exact solution within $[S^-, S^+]$ should not vary drastically between two successive timestamps. Second, we propose to use the signal passing in each interval at the point furthest from signals mean over the whole time frame. An algorithm that allows building such signal is given in Algorithm 3. Such signal is plotted in Figure 4(b).

5 Numerical assessment: example of an offshore wind substation

5.1 Description of the structure

The substation is a critical component of an offshore wind farm as it gathers electrical power from wind turbines and exports it to shore through a single cable. Therefore, assessing accurately its structural reliability is paramount. Let us consider an offshore wind substation designed by Chantiers de l'Atlantique. The monopile layout is represented in Figure 5 and supports a 2 500 metric ton (mT) topside that is represented in Figure 1. We consider that this structure is deployed by 30 m water depth at SEM-REV test site close to Le Croisic in France. The structure is considered to be made of steel with standard material properties: density $\rho = 7\,800 \text{ kg/m}^3$, Young modulus $E = 210 \text{ GPa}$, and Poisson coefficient $\nu = 0.3$. A single sea state modeled as a JON-SWAP spectrum is simulated as a unidirectional superimposition of 50 airy waves with random phases. The topside being symmetrical and the arm being more sollicitated by waves coming from \vec{e}_x than from \vec{e}_y , waves propagation ac-

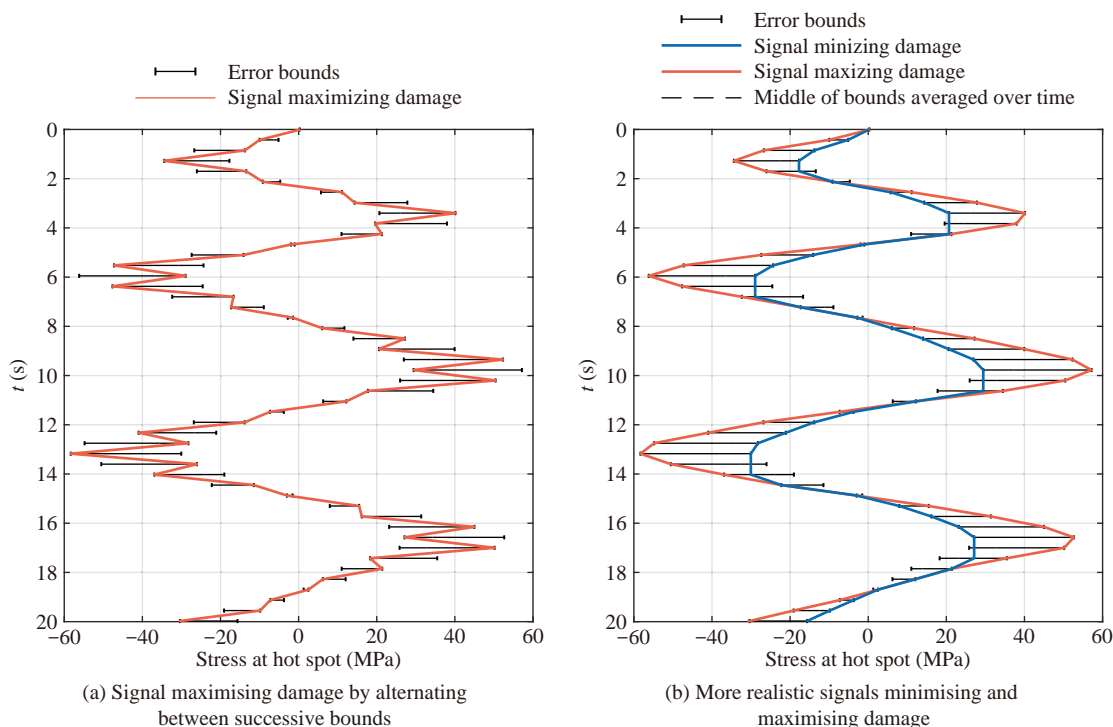


Figure 4 Signals maximizing and minizing fatigue damage

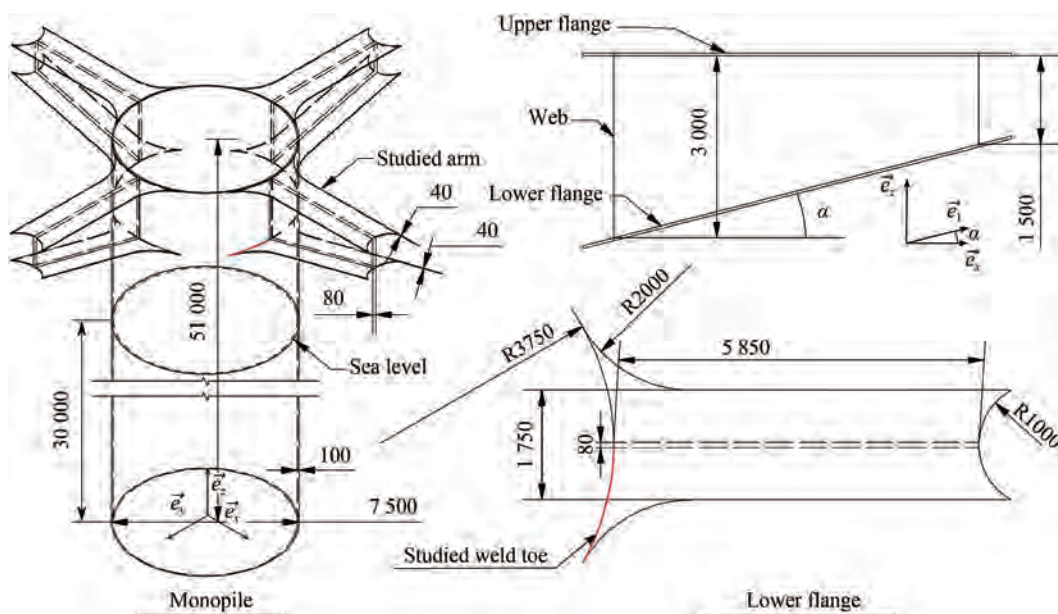


Figure 5 Offshore wind substation layout (Unit: mm)

According to \vec{e}_x is selected. The most probable sea state at the deployment site according to Ducroz et al. (2017) is chosen: $H_s = 2$ m, $T_p = 8.5$ s. We consider the fatigue failure under dynamical wave loads of the weld toe between the monopile and an arm aligned with wave propagation (see Figure 5). A two scale approach is used. First, a monopile mechanical problem is solved using dynamical beam theory to obtain loads close to the studied arm. Then a quasi-

static local lower flange mechanical problem allows computing local stress at the studied weld toe (see Figure 5). The discretization error is only measured on the local mechanical problem to avoid the use of a dynamical discretization error estimator Waeytens et al. (2012) that is not available in the homemade FEM code used in this paper.

Monopile mechanical problem First, only the monopile structure of the offshore substation (see Figure 6) is

modeled. Wave loads are computed through Morison equation (Sarpkava, 1986) according to the stochastic modeling in Schoefs (2008); Schoefs & Boukinda (2010) and following recommended practices from Veritas (2014). The structure is considered to be fully fixed to the ground on the one end and supports a 2 500 mT inertia on the other end. The structure is modeled using dynamical beam theory. The resulting discretized mechanical problem is:

$$\underline{\underline{M}} \frac{\partial^2 \underline{U}}{\partial t^2} (t) + \underline{\underline{K}} \underline{U} (t) = \underline{F} (t) \quad (19)$$

where \underline{U} contains 2D nodal displacements, $\underline{\underline{M}}$ contains inertia coefficients including the topside weight, $\underline{\underline{K}}$ is the stiffness matrix and $\underline{F}(t)$ is the wave load on the structure. The structure is discretized into 100 element which is a compromise between a small discretization error and a good condition number of the matrix $\underline{\underline{M}}$.

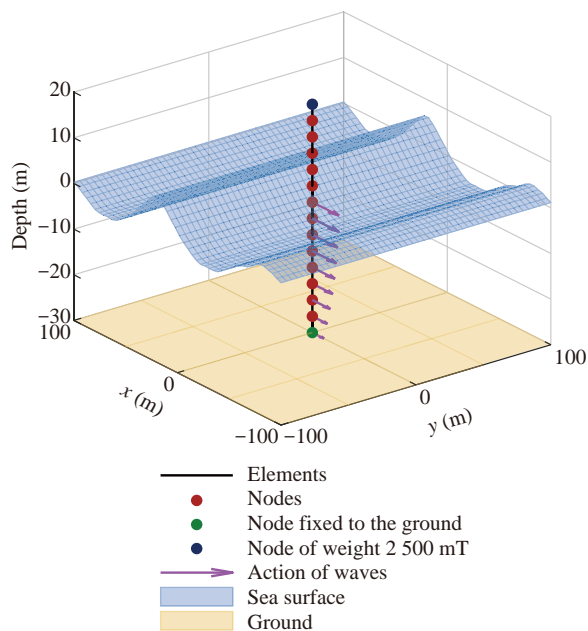


Figure 6 Monopile mechanical problem layout

The mechanical problem is solved for a 3 h sea state with a time discretization of $T_p / 20 = 0.425$ s using ode15 s in MATLAB®. The quantity of interest is σ_{11} at the closest node to the lower flange of the studied arm (see Figure 5) that governs fatigue computation.

Lower flange mechanical problem Second, the fatigue failure of the weld toe represented in Figure 5 is studied. In particular the point of the weld toe that is the closest to the beam web is selected as it is suspected to concentrate stress and be subjected to fatigue. For this problem $\sigma_{\perp} = \sigma_{11}$, $\sigma_{\parallel} = \sigma_{yy}$ and $\tau_{\parallel} = \sigma_{1y}$. Let us assume that $\sigma_{\perp} \gg \sigma_{\parallel}$, τ_{\parallel} . It implicates:

$$\sigma_1 = 1.12\sigma_{\perp} \quad (20)$$

Also, the hypothesis of 2D plane stress is made for the flange that is only subjected to loads from the monopile on the one end and is maintained fixed by the topside of the substation on the other end. As the mechanical problem is symmetrical both in terms of loads and geometry, only a single symmetric part of the flange is modeled. The resulting mechanical problem is represented in Figure 7. Recommended practices from Veritas (2010) suggest using a mesh size close to the zone of computation of the quantity of interest that is equal to the flange thickness that is 40 mm according to Figure 5. In order to reduce discretization error of both forward and adjoint problems at fixed computational cost, h-adaptivity Díez & Calderón (2007) is used. The resulting heterogenous mesh is shown in Figure 8 in which the mesh size close to the zone of computation of the quantity of interest is 11 mm.

5.2 Results and discussion

The method to compute bounds on the local stress σ_1 and propagate discretization error bounds toward fatigue damage is assessed on the offshore wind substation presented in 5.1. Two discretization error estimators are tested: one based on a stress smoothing technique (ZZ), one based on the error in constitutive relation and a flux free technique allowing the construction of an admissible stress field Parés et al. (2006) (ECR+FF).

5.2.1 Using ZZ error estimator

A 3 h time series of the finite element solution of σ_1 is obtained together with discretization error bounds using the ZZ estimator. A 20 s snippet of the time series is shown in Figure 9(a). The error intervals are very thin using that discretization error estimator so that the bounds cannot be seen without zooming (Figure 9(b)).

Once again, note that the ZZ error estimator provides error bounds that are not guaranteed. While they can be good indicators, bounds propagated toward fatigue damage or the probability of failure are therefore not guaranteed either. Then, the signals both minimizing and maximizing damage are built and the fatigue damage is computed for each of them together with the probability of failure (due to SN curve uncertainty) obtained by extrapolating the 3 h time series to 20 years of deployment. Results are given in Table 1. Two signals maximizing damage are tested: one passing the furthest from the 3 h mean of the finite element solution (Upp. bound in Table 1), one oscillating between upper and lower bound (Max. oscil. upp. bound. in Table 1). As the error interval on σ_1 is very thin, the interval is also thin on the 3 h fatigue damage and on the probability of failure. The upper bounds are fairly close using both methods. However, the upper bound using the signal passing the furthest from the 3 h mean of the FE solu-

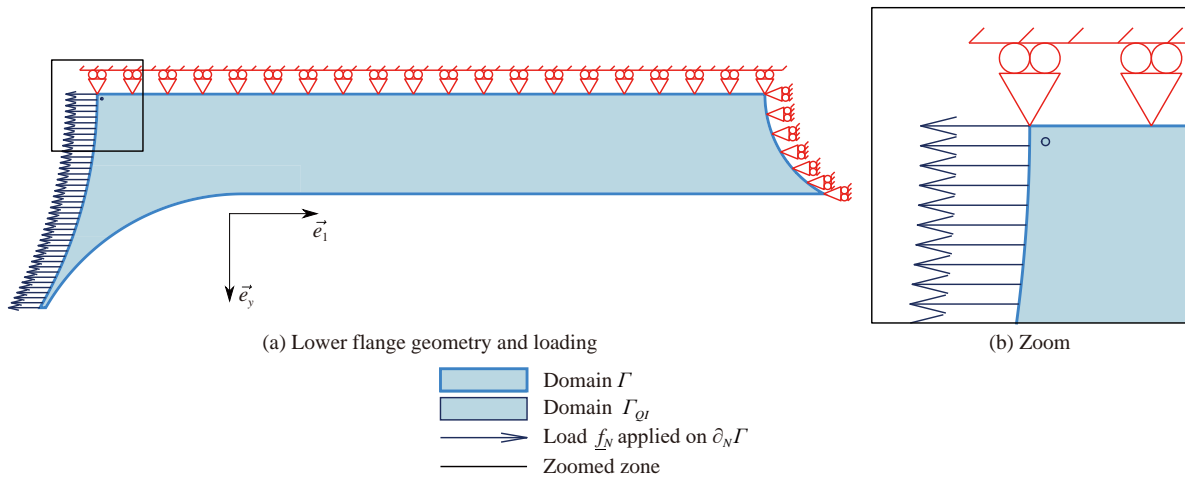


Figure 7 Lower flange mechanical problem

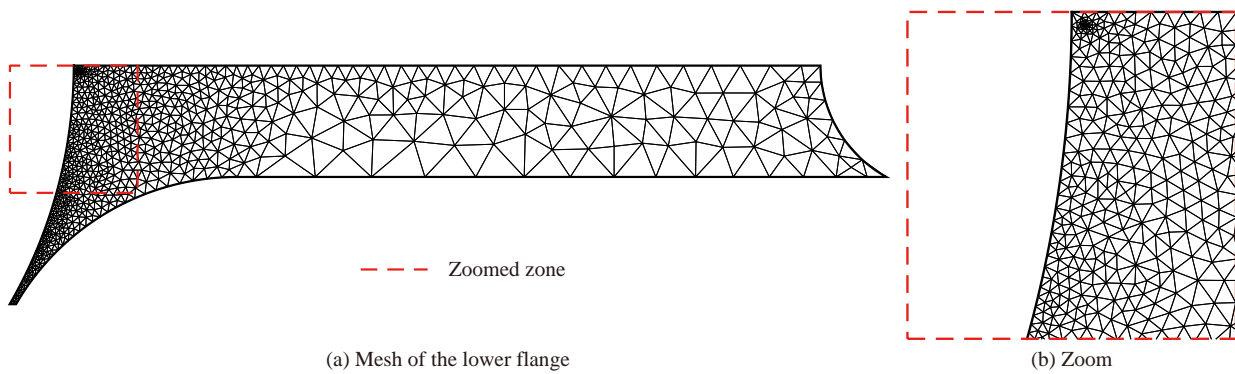


Figure 8 Mesh used for the lower flange mechanical problem

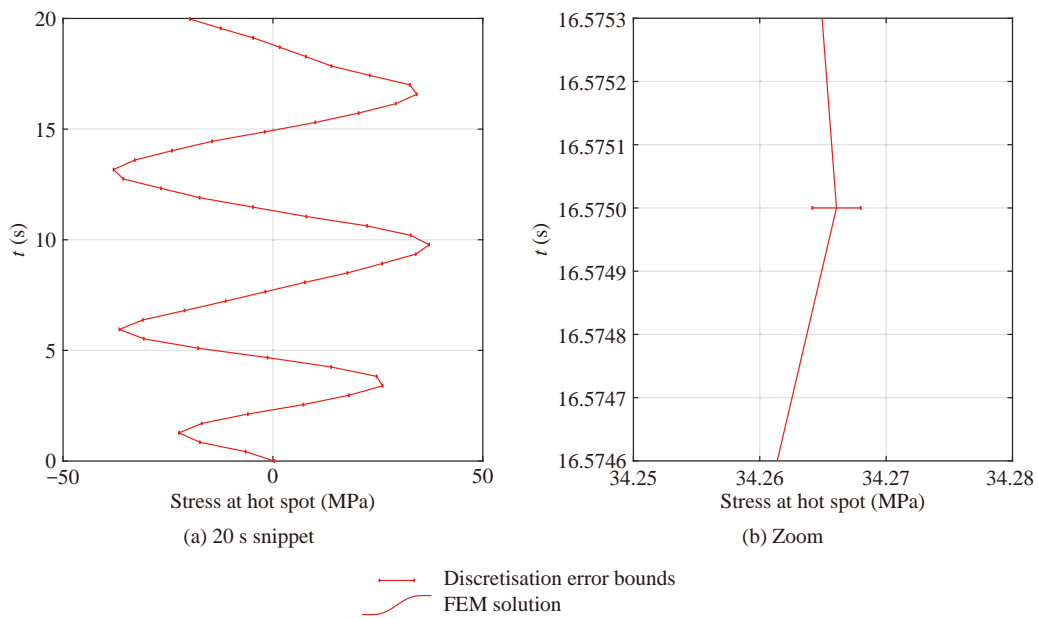


Figure 9 20 s snippet of the discretization error bounds time series obtained with the ZZ estimator

tion is slightly greater than the upper bound using the other signal maximizing damage. It is probably because the

signal oscillating between lower and upper bound is not guaranteed to pass the furthest from the 3 h mean at each

turning point. Even though this signal generates a lot of cy-

Table 1 Results using ZZ error estimator

	Low. bound	FEM solution	Upp. bound	Max. oscil. upp. bound
Damage in 3 h	1.17192×10^{-5}	1.17225×10^{-5}	1.17258×10^{-6}	1.17224×10^{-6}
P_f in 20 years	2.376×10^{-3}	2.380×10^{-3}	2.385×10^{-3}	2.380×10^{-3}

cles of small amplitude, those cycles do not have a significant contribution to the fatigue damage.

5.2.2 Using ECR+FF error estimator

A 3 h timeseries of discretization error bounds using the ERC+FF technique is also obtained. A 20 s snippet of that time series is plotted in Figure 10. First, the error intervals seem larger than with the ZZ estimator. Note that error bounds obtained with ECR+FF are guaranteed which make them more qualitative than error bounds obtain with ZZ.

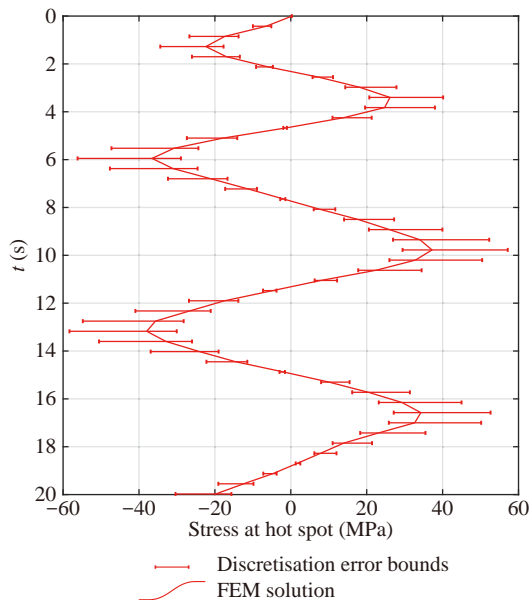


Figure 10 20 s snippet of the discretization error bounds time series obtained with the ECR+FF estimator

The error bounds on the fatigue damage and the probability of failure are given in Table 2. We can notice also that bounds using ZZ error estimators are included in the intervals obtained with ECR+FF estimators. While error bounds are large at turning points, the order of magnitude of the fatigue damage seems guaranteed by the error indicators. However, the error interval on the probability of failure is very large. If a smaller interval on the probability of failure was needed, turning points far from signals mean would need remeshing as only turning points are

used by rainflow counting and as a quasi-static framework is used. In a dynamical framework, the remeshing strategy would have to be more sophisticated as the precision at turning points depends also on the precision at previous time stamps. Also, the upper bound using the signal passing the furthest from the 3 h average is greater than the one obtained with the signal oscillating between lower and upper bounds. The error bounds being larger at turning points, the multitude of low amplitude cycles generated by the signal oscillating between lower and upper bounds creates less damage than a signal passing the furthest from the 3 h average at turning points. It seems to indicate that the signal passing in each interval the furthest from the 3h average is a greater majorizer of damage than the signal oscillating between lower and upper bounds.

Table 2 Results using ECR+FF error estimator

	Low. bound	FEM solution	Upp. bound	Max. oscil. upp. bound
Damage in 3 h	3.640×10^{-6}	1.172×10^{-5}	9.918×10^{-5}	8.612×10^{-5}
P_f in 20 years	4.107×10^{-8}	2.380×10^{-3}	0.965 2	0.934 2

6 Conclusion

A novel approach allowing to tackle discretization error in the damage assessment of offshore structures is introduced in this paper. By using a discretization error estimator, it is possible to obtain a time series of discretization error bounds for each sea state of the scatter diagram at the deployment site. We propose a method to propagate these error bounds to obtain bounds on the fatigue damage and the probability of failure of the structure. One signal minorizing damage while passing within error bounds at each time stamps is proposed. Two signals majorizing damage are proposed. The hypothesis on which these signals are built is that the more (respectively the less) a signal oscillates, the greater (respectively the smaller) the damage. While not being discussed, this hypothesis conforms with stress cycles identification through rainflow counting and SN curves. The first signal passes the furthest from the mean of the finite element solution. The second signal oscillates between lower and upper bounds at successive time stamps. The proposed method is assessed in a quasi-static framework on a beam flange of an offshore wind substation. Two estimators of the discretization error are tested. The first estimator uses a stress smoothing technique. It is available in some industrial FEM code but it is not guaranteed to give an upper bound on the discretization error. The second estimator is based on the error in constitutive relation. It is not available in industrial FEM codes but it provides a guaranteed upper bound on the dis-

cretization error. Results show that the ZZ estimator is not conservative and the second estimator should be implemented in industrial codes.

This method is implemented and illustrated for the fatigue assessment of a weld toe of an Offshore Wind Sub-Station. Results show that the signal passing the furthest from the mean of the signal seem to give a greater upper bound on damage than the other signal maximizing damage. It is therefore recommended to use the signal passing in each interval the furthest from the mean of the signal to compute an upper bound on the fatigue damage. It should be noted that it is not proved formally that the two signals proposed to respectively minimize and maximize fatigue damage allow obtaining guaranteed error bounds on the damage. Yet, it seems to be validated by experience for both error estimators.

The direction of the maximal principal stress was assumed in order to compute error bounds on this quantity of interest. Future works should focus on either linearizing maximal principal stress with regards to the displacement field or providing a specific method to obtain guaranteed error bounds for this quantity of interest.

This paper provides a complete framework for assessing rationally the FE error that can lead to bad decisions in the context of fatigue assessment on which relies inspection planing and digital twins of marine structures. Note that the method to propagate bounds toward damage may be used for other sources of uncertainty. For example, it allows computing the error on the local damage from a monitoring system of the nominal strain close to this point.

Appendix Algorithms

Algorithm 1 Build the signal minimizing damage

Require: S^- and S^+

$i = 1$

while $i \leq n_{ts}$ and $(S(t_0) < S^-(t_i) < S^+(t_0)$ or $S^-(t_0) < S^-(t_i) < S^+(t_0))$

$i = i + 1$

end while

if $S^+(t_0) < S^-(t_i)$ **then**

$S^{mini}(t_0) = S^+(t_0)$

else if $S^-(t_0) \geq S^+(t_i)$ **then**

$S^{mini}(t_0) = S^-(t_0)$

end if

for $i = 2 : n_{ts}$ **do**

if $S^-(t_i) < S^{mini}(t_{i-1}) < S^+(t_i)$ **then**

$S^{mini}(t_i) = S^{mini}(t_{i-1})$

else if $S^{mini}(t_{i-1}) \leq S^-(t_i)$ **then**

$S^{mini}(t_i) = S^-(t_i)$

else

$S^{mini}(t_i) = S^+(t_i)$

end if

end for

return S^{mini}

Algorithm 2 Build the signal maximizing damage by alternating between lower and upper bounds

Require: S^- and S^+

for $i = 1 : n_{ts}$ **do**

if i is odd **then**

$S^{maxi}(t_i) = S^-(t_i)$

else

$S^{maxi}(t_i) = S^+(t_i)$

end if

end for

return S^{maxi}

Algorithm 3 Build the signal maximizing damage by passing the furthest from FEM average signal

Require: S^-, S^+, S^{FEM}

$S_{avg} = \text{mean}(S^{FEM})$

for $i = 1 : n_{ts}$ **do**

if $|S^+(t_i) - S_{avg}| > |S^-(t_i) - S_{avg}|$ **then**

$S^{maxi}(t_i) = S^+(t_i)$

else

$S^{maxi}(t_i) = S^-(t_i)$

end if

end for

return S^{maxi}

Funding This work was carried out within the project MUSCAS (Multi-SCALE Stochastic computation for MRE) granted by WEAMEC, West Atlantic Marine Energy Community with the support of Région Pays de la Loire and in partnership with Chantiers de l'Atlantique.

References

- Ainsworth M & Oden J (1997) A posteriori error estimation in finite element analysis. *Computer methods in applied mechanics and engineering* 142(1-2): 1-88. [https://doi.org/10.1016/S0045-7825\(96\)01107-3](https://doi.org/10.1016/S0045-7825(96)01107-3)
- Alvin K (2000) Method for treating discretization error in nondeterministic analysis. *AIAA journal* 38(5): 910-916. <https://doi.org/10.2514/6.1999-1611>
- Becker R & Rannacher R (1996) A feed-back approach to error control in finite element methods: Basic analysis and examples. IWR
- Bitner-Gregersen E (2015) Joint met-ocean description for design and operations of marine structures. *Applied Ocean Research* 51: 279-292. <https://doi.org/10.1016/j.apor.2015.01.007>
- Casciati F, Colombi P & Faravelli L (1992) Fatigue lifetime evaluation via response surface methodology. In *European safety and reliability conference '92* (pp. 157-166)
- Demeyer S, Fischer N & Marquis D (2017) Surrogate model based sequential sampling estimation of conformance probability for computationally expensive systems: application to fire safety science. *Journal de la société française de statistique* 158(1): 111-138
- Díez P & Calderón G (2007) Remeshing criteria and proper error representations for goal oriented h-adaptivity. *Computer methods in applied mechanics and engineering* 196(4-6): 719-733. <https://doi.org/10.1016/j.cma.2006.03.005>

- Dong Y, Teixeira A & Soares CG (2018) Time-variant fatigue reliability assessment of welded joints based on the ϕ^2 and response surface methods. *Reliability Engineering & System Safety* 177: 120-130. <https://doi.org/10.1016/j.res.2018.05.005>
- Ducrozet G, Bonnefoy F & Perignon Y (2017) Applicability and limitations of highly nonlinear potential flow solvers in the context of water waves. *Ocean Engineering* 142: 233-244. <https://doi.org/10.1016/j.oceaneng.2017.07.003>
- Gallimard L (2011) Error bounds for the reliability index in finite element reliability analysis. *International journal for numerical methods in engineering* 87(8): 781-794. <https://doi.org/10.1002/nme.3136>
- Ghavidel A, Mousavi S & Rashki, M (2018) The effect of FEM mesh density on the failure probability analysis of structures. *KSCE Journal of Civil Engineering* 22(7): 2370-2383. <https://doi.org/10.1007/s12205-017-1437-5>
- Ghavidel A, Rashki M, Arab H & Moghaddam M (2020) Reliability mesh convergence analysis by introducing expanded control variates. *Frontiers of Structural and Civil Engineering* 14(4): 1012-1023. <https://doi.org/10.1007/s12205-017-1437-5>
- Huchet Q, Mattrand C, Beaurepaire P, Relun N & Gayton N (2019) AK-DA: An efficient method for the fatigue assessment of wind turbine structures. *Wind Energy* 22(5): 638-652. <https://doi.org/10.1002/we.2312>
- Ladevèze P (2006) Upper error bounds on calculated outputs of interest for linear and nonlinear structural problems. *Comptes Rendus Académie des Sciences -Mécanique, Paris* 334(7): 399-407. <https://doi.org/10.1016/j.crme.2006.04.004>
- Ladevèze P (2008, 01) Strict upper error bounds on computed outputs of interest in computational structural mechanics. *Computational Mechanics* 42(2): 271-286. <https://doi.org/10.1007/s00466-007-0201-y>
- Ladevèze P & Leguillon D (1983) Error estimate procedure in the finite element method and applications. *SIAM Journal on Numerical Analysis* 20(3): 485-509. <https://doi.org/10.1137/0720033>
- Ladevèze P & Pelle J-P (2005) *Mastering calculations in linear and nonlinear mechanics* (Vol. 171). Springer
- Matsuishi M & Endo T (1968) *Fatigue of metals subjected to varying stress*. Japan Society of Mechanical Engineers, Fukuoka, Japan 68(2): 37-40
- Mell L, Rey V & Schoefs F (2020) Multifidelity adaptive kriging metamodel based on discretization error bounds. *International Journal for Numerical Methods in Engineering* 121(20): 4566-4583. <https://doi.org/10.1002/nme.6451>
- Parés N, Díez P & Huerta A (2006) Subdomain-based flux-free posteriori error estimators. *Computer Methods in Applied Mechanics and Engineering* 195(4-6): 297-323. <https://doi.org/10.1016/j.cma.2004.06.047>
- Paris PC (1961) A rational analytic theory of fatigue. *Trends Engin* 13: 9-14
- Pasqualini O, Schoefs F, Chevreuil M & Cazuguel M (2013) Measurements and statistical analysis of fillet weld geometrical parameters for probabilistic modelling of the fatigue capacity. *Marine structures* 34: 226-248. <https://doi.org/10.1016/j.marstruc.2013.10.002>
- Pled F, Chamoin L & Ladevèze P (2011) On the techniques for constructing admissible stress fields in model verification: Performances on engineering examples. *International Journal for Numerical Methods in Engineering* 88(5): 409-441. <https://doi.org/10.1002/nme.3180>
- Rey V, Gosselet P & Rey C (2014) Study of the strong prolongation equation for the construction of statically admissible stress fields: implementation and optimization. *Computer Methods in Applied Mechanics and Engineering* 268: 82-104. <https://doi.org/10.1016/j.cma.2013.08.021>
- Rüter M & Stein E (2006) Goal-oriented posteriori error estimates in linear elastic fracture mechanics. *Computer methods in applied mechanics and engineering* 195(4-6): 251-278. <https://doi.org/10.1016/j.cma.2004.05.032>
- Sarpkaya T (1986) Force on a circular cylinder in viscous oscillatory flow at low keulegan—carpenter numbers. *Journal of Fluid Mechanics* 165: 61-71. <https://doi.org/10.1017/S0022112086002999>
- Schoefs F (2008) Sensitivity approach for modelling the environmental loading of marine structures through a matrix response surface. *Reliability Engineering & System Safety* 93(7): 1004-1017. <https://doi.org/10.1016/j.res.2007.05.006>
- Schoefs F & Boukinda ML (2010) Sensitivity approach for modeling stochastic field of keulegan- carpenter and reynolds numbers through a matrix response surface. *Journal of offshore mechanics and Arctic engineering* 132(1). <https://doi.org/10.1115/1.3160386>
- Soares CG & Garbatov Y (1996) Fatigue reliability of the ship hull girder accounting for inspection and repair. *Reliability Engineering & System Safety* 51(3): 341-351. [https://doi.org/10.1016/0951-8320\(95\)00123-9](https://doi.org/10.1016/0951-8320(95)00123-9)
- Strouboulis T, Babuška I, Datta D, Copps K & Gangaraj S (2000) A posteriori estimation and adaptive control of the error in the quantity of interest. part i: A posteriori estimation of the error in the von mises stress and the stress intensity factor. *Computer Methods in Applied Mechanics and Engineering* 181(1-3): 261-294. [https://doi.org/10.1016/S0045-7825\(99\)00077-8](https://doi.org/10.1016/S0045-7825(99)00077-8)
- Veritas DN (1996) Guidelines for offshore structural reliability analysis—application to jacket platforms (Tech. Rep.). DNV Report.
- Veritas DN (2010) DNV-RP-C203 fatigue design of offshore steel structures. DNV, Baerum, Norway.
- Veritas DN (2014) Dnv-rp-c205: Environmental conditions and environmental loads (Tech. Rep.). DNV GL
- Waeytens J, Chamoin L & Ladevèze P (2012) Guaranteed error bounds on pointwise quantities of interest for transient viscodynamics problems. *Computational Mechanics* 49(3): 291-307. <https://doi.org/10.1007/s00466-011-0642-1>
- Zienkiewicz O & Zhu J (1987) A simple error estimator and adaptive procedure for practical engineering analysis. *International journal for numerical methods in engineering* 24(2): 337-357. <https://doi.org/10.1002/nme.1620240206>